IEEE Access
Multidisciplinary ⋮ Rapid Review ⋮ Open Access Journal

Received 30 November 2023, accepted 25 December 2023, date of publication 28 December 2023,
date of current version 2 February 2024.

Digital Object Identifier 10.1109/ACCESS.2023.3347810

RESEARCH ARTICLE

O_2 Plasma Alternately Treated ALD-Al_2O_3 as Gate Dielectric for High Performance AlGaN/GaN MIS-HEMTs

QIANG WANG, MAOLIN PAN, PENGHAO ZHANG, LUYU WANG, YANNAN YANG, XINLING XIE, HAI HUANG, XIN HU, AND MIN XU
State Key Laboratory of ASIC and System, School of Microelectronics, Fudan University, Shanghai 200433, China
Corresponding author: Min Xu (xu_min@fudan.edu.cn)

ABSTRACT This article systematically studies the AlGaN/GaN MIS-HEMTs using the O_2 plasma alternately treated Al_2O_3 as gate dielectric. The X-ray photoelectron spectroscopy (XPS) analyses and capacitance-voltage (C-V) measurement results show that the density of the border traps originating from the Al-OH bonds in the ALD-Al_2O_3 gate dielectric can be significantly reduced after the O_2 plasma alternating treatment. Consequently, a low gate leakage current and a high field-effect mobility of $1680 cm^2/V\cdot s$ are achieved. The results also demonstrate that the fabricated AlGaN/GaN MIS-HEMTs with the O_2 plasma alternating treatment exhibit improved performances, having a high ON/OFF ratio of $\sim 10^{11}$, a steep subthreshold slope of 74 mV/dec, a small hysteresis (ΔV_{TH}) of 0.1 V and small ON-resistance (R_{ON}) of 6.0 Ω·mm. The device thermal stability was also improved within the tested temperature range. In addition, the pulsed I_D-V_{DS} measurements with quiescent drain bias (V_{DS0}) stress of 40 V present negligible current collapse (2%) and low degradation of dynamic R_{ON} by 1.04 times the static R_{ON}.

INDEX TERMS AlGaN/GaN MIS-HEMTs, border traps, current collapse, plasma alternately treated gate dielectric.

I. INTRODUCTION

The AlGaN/GaN-based high-electron-mobility transistors (HEMTs) with metal–insulator–semiconductor (MIS) structures have been expected to be used in the next-generation power switching applications due to their favorable material characteristics, including high electron mobility, low on-resistances, and high critical breakdown electric field [1], [2], [3], [4]. The MIS structures can effectively suppress the gate leakage current and increase the gate swing compared to the conventional Schottky-gate HEMTs (S-HEMTs). Various high-k materials, including Al_2O_3 [5], HfO_2 [6], AlN [7], SiN_x [8] and SiO_2 [9], have been used as gate dielectrics for the AlGaN/GaN MIS-HEMTs in recent studies. Among them, Al_2O_3 has been the most preferable due to its large dielectric constant, high breakdown electric field ($\sim$10 MV/cm) and a large bandgap and conduction band offset to (Al)GaN [10], [11], [12].

The atomic layer deposition (ALD) Al_2O_3 film using trimethylaluminum (TMA) and water as precursors contains a large number of hydroxyl (-OH) groups, which is associated with the border traps in the gate dielectric. To reduce the density of -OH groups in Al_2O_3, related studies have proposed using ozone as the oxidant [13], [14], [15]. However, using ozone as the oxygen precursor might increase the carbon (C) content in the Al_2O_3 film due to its high reaction activity [16], [17]. Ryohei et al. reported suppressed electrical defects in Al_2O_3 film by incorporation nitrogen into Al_2O_3 [18], but dielectric constant has decreased. Wang et al. [19] demonstrated high quality Al_2O_3 film can be obtained by utilizing H_2O and O_2 plasma as oxidants in each cycle. However, the O_2 plasma could cause damage to the AlGaN surface during the early stages of Al_2O_3 film deposition [20]. To address the aforementioned limitation, this study proposes the O_2 plasma alternately treated Al_2O_3 to improve the Al_2O_3 quality. The

The associate editor coordinating the review of this manuscript and approving it for publication was Guangcun Shan.

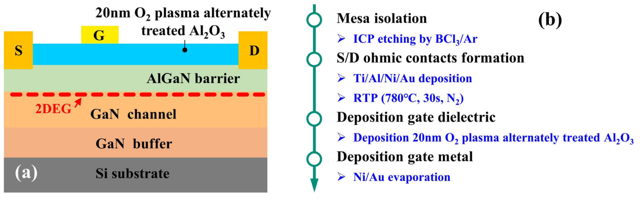

FIGURE 1. (a) The cross-sectional schematic of the fabricated AlGaN/GaN MIS-HEMTs. (b) The corresponding key process flow.

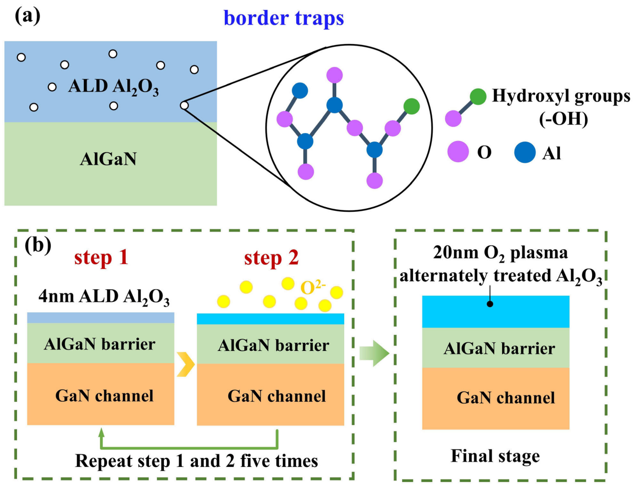

FIGURE 2. (a) Schematic diagram of the border traps in the ALD-Al_2O_3 gate dielectric. (b) The process flow charts of depositing the O_2 plasma alternately treated Al_2O_3 gate dielectric.

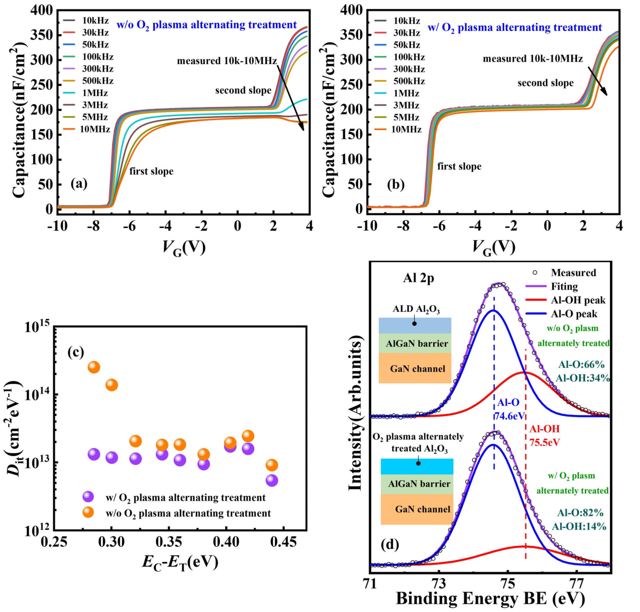

FIGURE 3. The multi-frequency C–V characteristics of the MIS diode with measurement frequency f_m varying from 10 kHz to 10MHz (a) without and (b) with O_2 plasma alternating treatment. (c) Distribution of trap density of the MIS diode. (d) XPS spectroscopy of the Al 2p peak of the Al_2O_3 film without (Upper) and with (under) O_2 plasma alternating treatment.

results indicate that the Al_2O_3 with the O_2 plasma alternating treatment can reduce the border trap density, yielding excellent device performances.

II. DEVICE STRUCTURE AND FABRICATION

The cross-sectional schematic of the fabricated AlGaN/GaN MIS-HEMTs is shown in Fig. 1(a). The sample used in this work was comprised of a 5-μm carbon-doped GaN buffer layer, a 180-nm GaN channel layer, and a 20-nm $Al_{0.25}Ga_{0.75}N$ barrier layer. The corresponding key process flow is illustrated in Fig. 1(b). The mesa isolation region was formed by the BCl_3/Ar gas inductively coupled plasma (ICP) etching. The ohmic contact was formed using Ti/Al/Ni/Au metal stack, followed by rapid thermal annealing at 780°C for 30 s in nitrogen ambient. The contact resistance was measured to be 1 Ω·mm using transfer length method (TLM).

As shown in Fig. 2(a), there were high-density border traps in the Al_2O_3 gate dielectric due to the incomplete reaction of the TMA and water precursors. The O_2 plasma alternating treatment was used to reduce the border traps in the Al_2O_3. The process flow charts of depositing the O_2 plasma alternately treated Al_2O_3 gate dielectric is presented in Fig. 2(b). First, a 4-nm ALD-Al_2O_3 film was deposited using the TMA and water as precursors in Sentech SI ALD system at the substrate temperature of 300 °CC. Then, in situ O_2 plasma treatment was performed with 100 sccm O_2 gas flow, 15 Pa gas pressure and a plasma power of 100 W for 2 min at 300 °C. Finally, the first and second steps were repeated five times. Afterwards, a 20-nm plasma alternately treated Al_2O_3 gate dielectric was obtained. It should be noted that if the deposited Al_2O_3 film in the first step was too thin, the O_2 plasma could cause damage to the (Al)GaN surface [21]. Finally, 40/200nm Ni/Au gate electrodes were deposited and patterned after the source and drain via opening. The device without O_2 plasma alternately treated Al_2O_3 gate dielectric was also prepared and served as a reference device. The gate-to-source spacing L_{GS}, gate length L_G and gate-to-drain spacing L_{GD} were 4-μm, 2-μm, and 6-μm, respectively.

III. DEVICE CHARACTERISTICS AND DISCUSSION

The distribution of border traps was characterized using the C–V measurement of the MIS diode fabricated on the same wafer. The obtained C–V curves had two slopes, the first slope was at a negative voltage corresponded to the formation of the 2DEG channel, and the second slope was at a positive voltage corresponded to the spill-over of the 2DEG. The device without the O_2 plasma alternating treatment exhibited large frequency dispersions due to the existence of border traps, as shown in Fig. 3(a). In contrast, for the device with the O_2 plasma alternating treatment, the frequency dispersions were every small, as presented in Fig. 3(b), which indicated that the border trap density was relatively low [22], [23]. The second slope onset voltage frequency-dependent shift in the C–V curves was used to calculate the distribution of border traps as follows [24], [25]:

$$\mathrm{D}_{it} = (E_C - E_T = \Delta E_{T\_AVG}) = \frac{C_{ox}\Delta V_{ON}}{q \cdot \Delta E_{dis}} - \frac{C_{ox} + C_B}{q^2} \quad (1)$$

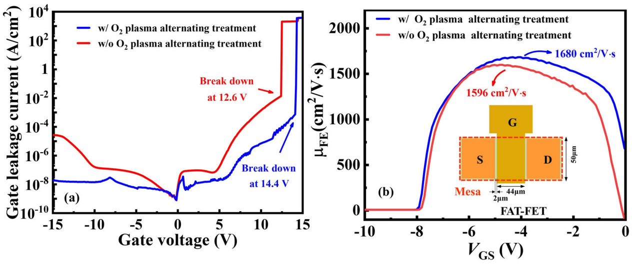

FIGURE 4. (a) The gate leakage current as a function of the voltage biases. (b) The field-effect mobility extracted from the FAT-FET for the samples with and without the O_2 plasma alternating treatment.

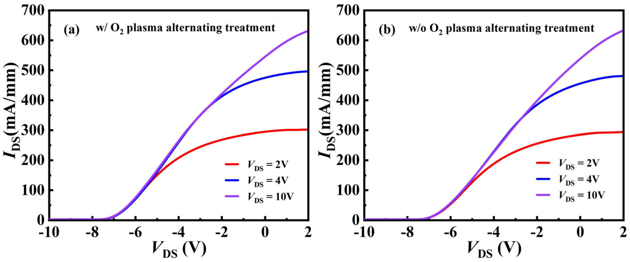

FIGURE 5. Transfer curves measured at various VDS values of 2, 4, and 10 V in the linear scale for the samples with and without the O2 plasma alternating treatment.

where q is the electron charge; C_{ox} is the dielectric capacitance; C_B is the barrier layer capacitance; ΔE_{dis} is differences in energy levels at different measurement frequencies; ΔV_{ON} is the onset voltage frequency-dependent shift.

The distribution of border trap density (D_{it}) obtained by (1) is presented in Fig. 3(c). For the sample with the O_2 plasma alternating treatment, varied from 5×10^{12} cm^{-2} eV^{-1} to 1.6×10^{13} cm^{-2} eV^{-1} in the energy level range of 0.28-0.45 eV below the conduction band edge, which was a fairly low trap density compared to the up-to-date reported data [26], [27], [28]. However, the sample without the O_2 plasma alternating treatment exhibited high trap density especially within the range of shallow energy levels. The XPS was performed on the Al_2O_3 sample both with and without the O_2 plasma alternating treatment to investigate the origin of border traps in the Al_2O_3. The measured binding energy was calibrated by correcting the adventitious C 1s peak to 284.8 eV. The Al 2p peak could be decomposed into two components: the Al–OH bond at 75.5 eV and the Al–O bond at 74.6 eV. As shown in Fig. 3(d), the content of Al–OH bonds was significantly reduced, indicting the Al–OH bonds were the main cause of border traps in the ALD-Al_2O_3 film [15], [29].

Fig. 4(a) shows the gate leakage current density versus the voltage biases of the MIS diodes. The MIS diode with the O_2 plasma alternating treatment exhibited a well-suppressed gate leakage current density of 6.1×10^{-6} A/cm^2 at a forward bias of 10 V compared to the gate leakage current density of 1.1×10^{-3} A/cm^2 of the sample without the O_2 plasma alternating treatment. The forward breakdown voltage values of the samples with and without the O_2 plasma alternating treatment were 14.4 V and 12.6 V, respectively. The reduction in the leakage current and the increase in the forward breakdown voltage further proved that the gate dielectric has high quality after the O_2 plasma alternating treatment.

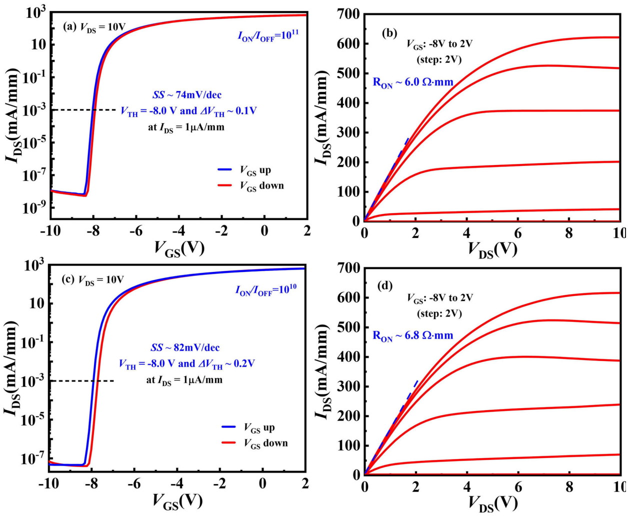

FIGURE 6. The transfer (left) and output (right) characteristics of the MIS-HEMTs (a)-(b) with and (c)-(d) without the O_2 plasma alternating treatment.

The effective mobility $\mu_{FE} = L_G G_m/(W_G C_{MIS} V_{DS})$ extracted from a long-channel MIS-HEMT (FAT-FET) [30] with the 44-μm L_G, 50-μm W_G, 2-μm L_{GS} and L_{GD} at V_{DS} = 0.1 V are shown in Fig. 4(b). The device with the O_2 plasma alternating treatment had a relatively higher μ_{FE} with a peak value of 1680cm^2/V·s. For comparison, the maximum field-effect mobility for the device without O_2 plasma alternating treatment was 1596 cm^2/V·s. The improved μ_{FE} indicated the suppressed remote scattering of the border traps [31], [32].

Fig. 5 showed the transfer curves measured at various V_{DS} values of 2, 4, and 10 V for the devices with and without the O_2 plasma alternating treatment, suggesting both devices have stable threshold voltages (V_{TH}) at different V_{DS} in the linear scale. To facilitate the calculation of threshold hysteresis (ΔV_{TH}) and ON/OFF ratio, the semilog scale was used to defined V_{TH} at I_{DS} of 1 μA/mm in the upsweep measurement.

As shown in Fig. 6, the transfer and output characteristics of the MIS-HEMTs with the O_2 plasma alternating treatment yielded a small ΔV_{TH} of ~0.1 V, steep subthreshold slope (SS) of ~74 mV/dec, high ON/OFF ratio (I_{ON}/I_{OFF}) in the order of ~10^{11} and small ON-resistance (R_{ON}) of 6.0 Ω·mm. For comparison, the MIS-HEMTs without the O_2 plasma alternating treatment exhibited a larger ΔV_{TH} of ~0.2 V, *SS* of ~ 82 mV/dec, lower I_{ON}/I_{OFF} ratio of ~10^{10} and larger R_{ON} of 6.8 Ω·mm. The improved R_{ON} of the device with the O_2 plasma alternating treatment could be attributed to the increase in μ_{FE} mentioned above.

The transfer and output characteristics comparison of the MIS-HEMT at RT (30°C) and 150 °C were characterized in Fig. 7. When the temperature was raised up to 150°C, the

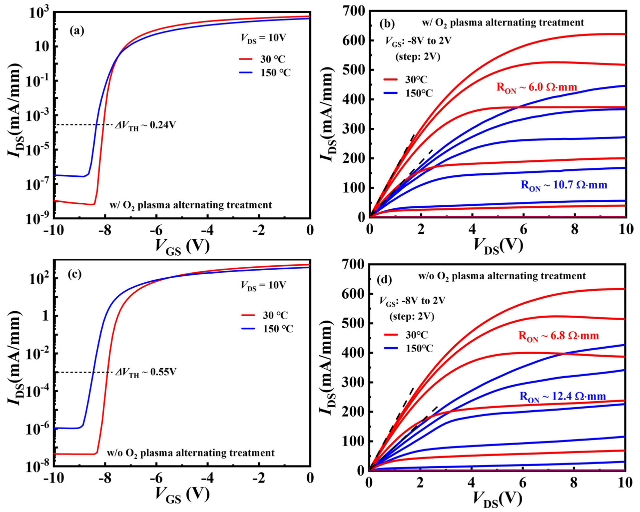

FIGURE 7. The transfer (left) and output (right) characteristics of the MIS-HEMTs at RT and 150°C (a)-(b) with and (c)-(d) without the O_2 plasma alternating treatment.

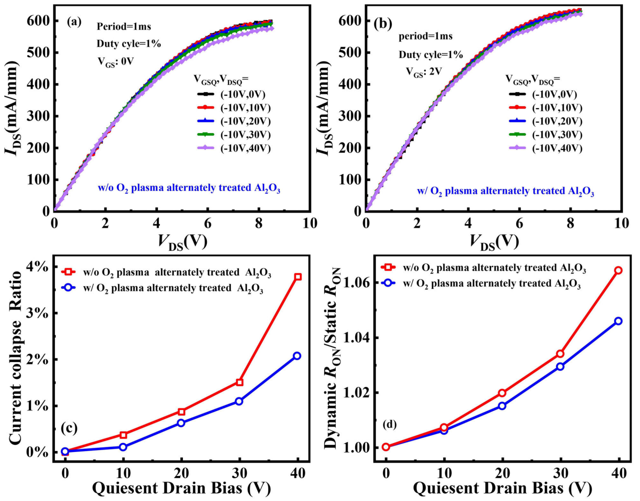

FIGURE 8. The pulsed I_D V_{DS} characteristics of the AlGaN/GaN MIS-HEMT with various quiescent biases (a) with and (b) without the O_2 plasma alternating treatment. (c)-(d) The current collapse and dynamic R_{ON} at different quiescent drain bias.

thermal shifts of V_{TH} were 0.24 V and 0.55 V for the device with and without the O_2 plasma alternating treatment, respectively. Moreover, The R_{ON} increased from 6.0 Ω·mm to 10.7 Ω·mm and from 6.8 Ω·mm to 12.4 Ω·mm for the device with and without the O_2 plasma alternating treatment, respectively. The device also exhibited improved thermal stability that is attributed to the high-quality gate dielectric.

A pulsed I_D-V_{DS} measurement with different quiescent drain bias (V_{DS0}) was performed to evaluate the dynamic performance of the device [33]. The pulse period was set to 1-ms with a duty cycle of 1%. The maxima value of V_{DS0} was limited to 40 V because of the transient high power and current during the hard switch. During the pulsed I_D-V_{DS} measurement, the gate quiescent voltage (V_{GSQ}) was kept at OFF-state of 2V below the threshold voltage, and the drain quiescent voltage (V_{DSQ}) was varied from 0 to 40 V at V_{GS} = 0. The pulsed output current corresponding to ($V_{GSQ} = 0$ and $V_{DSQ} = 0$) was selected as the static state to eliminate the self-heating effects [34]. Fig. 8 shows the pulsed I_D-V_{DS} characteristics of the devices with and without the O_2 plasma alternating treatment. The current collapse ratio was evaluated as a decrease in I_{DS} at V_{DS} = 10 V, the dynamic R_{ON} was extracted from the linear region (V_{DS}: 0 to 1V) of the pulsed output curve. The current collapse ratio and the ratio of dynamic R_{ON} to static R_{ON} as a function of V_{DS0} are shown in Fig. 8(c) and 8(d), respectively. The dynamic R_{ON} and current collapse increased with higher V_{DS} stress due to the enhanced electron trapping in the border traps of the gate-dielectric [35], [36], [37]. The device with the O_2 plasma alternating treatment suppressed the degradation of dynamic R_{ON} by 1.04 times the static R_{ON} at the V_{DS0} stress of 40 V, and dynamic R_{ON} was 1.06 times the static R_{ON} for the device without the O_2 plasma alternating treatment. Similarly, a negligible current collapse (~2%) was observed for the devices with the O_2plasma alternating treatment at the V_{DS0} stress of 40 V, whereas the devices without the O_2 plasma alternating treatment showed a larger current collapse (~4%) at the same V_{DS0} stress.

TABLE 1. Performance comparison of different treatment methods for Al_2O_3.

	Bias annealing at 300°C	PDA at 700°C	Using ozone as precursor	O_2 plasma alternating treatment
D_{it} ($cm^{-2}eV^{-1}$)	2×10^{12}- 1×10^{13}	4×10^{12}- 2×10^{13}	-	5×10^{12}- 1.6×10^{13}
ΔV_{TH} (V)	-	0.5	0.12	0.1
R_{ON} (Ω·mm)	-	-	-	6.0
SS (mV/dec)	112	-	73	74
References	[38]	[39]	[40]	This Work

Table 1 showed the key characteristics of different treatment methods for Al_2O_3 in the literature. The device employing the O_2 plasma alternating treatment exhibited the most improved result in overall performances, which indicated that it is an effective method to improve the quality of gate dielectric.

IV. CONCLUSION

In this study, the O_2 plasma alternately treated Al_2O_3 technique is proposed to reduce the border trap density in the gate dielectric. The off-state leakage current, ΔV_{TH}, SS, I_{ON}/I_{OFF} ratio, R_{ON} and the thermal stability are improved, and the dynamic R_{ON} and current collapse are suppressed in the AlGaN/GaN MIS-HEMTs with the O_2 plasma alternating treatment. These analysis results indicate that the O_2 plasma alternating treatment technique could be an effective approach for fabricating high performance GaN-on-Si HEMTs for power device applications.

REFERENCES

[1] M. Ishida, T. Ueda, T. Tanaka, and D. Ueda, "GaN on Si technologies for power switching devices," *IEEE Trans. Electron Devices*, vol. 60, no. 10, pp. 3053–3059, Oct. 2013, doi: 10.1109/TED.2013.2268577.

[2] K. J. Chen, O. Häberlen, A. Lidow, C. L. Tsai, T. Ueda, Y. Uemoto, and Y. Wu, "GaN-on-Si power technology: Devices and applications," *IEEE Trans. Electron Devices*, vol. 64, no. 3, pp. 779–795, Mar. 2017, doi: 10.1109/TED.2017.2657579.

[3] K. Deng, S. Huang, X. Wang, Q. Jiang, H. Yin, J. Fan, G. Jing, K. Wei, Y. Zheng, J. Shi, and X. Liu, "Insight into the suppression mechanism of bulk traps in Al_2O_3 gate dielectric and its effect on threshold voltage instability in Al_2O_3/AlGaN/GaN metal-oxide-semiconductor high electron mobility transistors," *Appl. Surf. Sci.*, vol. 638, Nov. 2023, Art. no. 158000, doi: 10.1016/j.apsusc.2023.158000.

[4] D. Bouguenna, A. Beloufa, K. Hebali, and S. A. Loan, "Investigation of the electrical characteristics of AlGaN/AlN/GaN heterostructure MOS-HEMTs with TiO_2 high-k gate insulator," *Int. J. Nanoelectron. Mater.*, vol. 16, no. 3, pp. 607–620, Jul. 2023.

[5] Z. H. Liu, G. I. Ng, S. Arulkumaran, Y. Maung, K. L. Teo, S. C. Foo, V. Sahmuganathan, T. Xu, and C. H. Lee, "High microwave-noise performance of AlGaN/GaN MISHEMTs on silicon with $Al_2Ø_3$ gate insulator grown by ALD," *IEEE Electron Device Lett.*, vol. 31, no. 2, pp. 96–98, Feb. 2010, doi: 10.1109/LED.2009.2036135.

[6] S. Abermann, G. Pozzovivo, J. Kuzmik, G. Strasser, D. Pogany, J.-F. Carlin, N. Grandjean, and E. Bertagnolli, "MOCVD of HfO_2 and ZrO_2 high-k gate dielectrics for InAlN/AlN/GaN MOS-HEMTs," *Semicond. Sci. Technol.*, vol. 22, no. 12, pp. 1272–1275, Dec. 2007, doi: 10.1088/0268-1242/22/12/005.

[7] S. Tan, S. L. Selvaraj, and T. Egawa, "Metal-organic chemical vapor deposition of quasi-normally-off AlGaN/GaN field-effect transistors on silicon substrates using low-temperature grown AlN cap layers," *Appl. Phys. Lett.*, vol. 97, no. 5, Aug. 2010, doi: 10.1063/1.3475394.

[8] M. Fagerlind, F. Allerstam, E. Ö. Sveinbjörnsson, N. Rorsman, A. Kakanakova-Georgieva, A. Lundskog, U. Forsberg, and E. Janzén, "Investigation of the interface between silicon nitride passivations and AlGaN/AlN/GaN heterostructures by C(V) characterization of metal-insulator-semiconductor-heterostructure capacitors," *J. Appl. Phys.*, vol. 108, no. 1, Jul. 2010, doi: 10.1063/1.3428442.

[9] H. Kambayashi, Y. Satoh, S. Ootomo, T. Kokawa, T. Nomura, S. Kato, and T.-S.-P. Chow, "Over 100A operation normally-off AlGaN/GaN hybrid MOS-HFET on Si substrate with high-breakdown voltage," *Solid-State Electron.*, vol. 54, no. 6, pp. 660–664, Jun. 2010, doi: 10.1016/j.sse.2010.01.001.

[10] A. Calzolaro, T. Mikolajick, and A. Wachowiak, "Status of aluminum oxide gate dielectric technology for insulated-gate GaN-based devices," *Materials*, vol. 15, no. 3, p. 791, Jan. 2022, doi: 10.3390/ma15030791.

[11] K. Y. Park, H. I. Cho, J. H. Lee, S. B. Bae, C. M. Jeon, J. L. Lee, D. Y. Kim, C. S. Lee, and J. H. Lee, "Fabrication of AlGaN/GaN MIS-HFET using an Al_2O_3 high k dielectric," in *Proc. 5th Int. Conf. Nitride Semiconductors (ICNS-5)*, Nara, Japan, 2003, pp. 2351–2354.

[12] Y. Yuan-Zheng, H. Yue, F. Qian, Z. Jin-Cheng, M. Xiao-Hua, and N. Jin-Yu, "GaN MOS-HEMT using ultra-thin Al_2O_3 dielectric grown by atomic layer deposition," *Chin. Phys. Lett.*, vol. 24, no. 8, pp. 2419–2422, Aug. 2007, doi: 10.1088/0256-307x/24/8/072.

[13] S. Huang, Q. Jiang, K. Wei, G. Liu, J. Zhang, X. Wang, and Y. Zheng, "High-temperature low-damage gate recess technique and ozone-assisted ALD-grown Al_2O_3 gate dielectric for high-performance normally-off GaN MIS-HEMTs," in *IEDM Tech. Dig.*, Dec. 2014, pp. 17.4.1–17.4.4.

[14] H. Tokuda, J. T. Asubar, and M. Kuzuhara, "AlGaN/GaN metal–insulator–semiconductor high-electron mobility transistors with high on/off current ratio of over 5×10^{10} achieved by ozone pretreatment and using ozone oxidant for Al_2O_3 gate insulator," *Jpn. J. Appl. Phys.*, vol. 55, no. 12, Dec. 2016, Art. no. 120305, doi: 10.7567/jjap.55.120305.

[15] M. Choi, A. Janotti, and C. G. Van de Walle, "Native point defects and dangling bonds in α-Al_2O_3," *J. Appl. Phys.*, vol. 113, no. 4, Jan. 2013, doi: 10.1063/1.4784114.

[16] T. Kubo, J. J. Freedsman, Y. Iwata, and T. Egawa, "Electrical properties of GaN-based metal–insulator–semiconductor structures with Al_2O_3 deposited by atomic layer deposition using water and ozone as the oxygen precursors," *Semicond. Sci. Technol.*, vol. 29, no. 4, Apr. 2014, Art. no. 045004, doi: 10.1088/0268-1242/29/4/045004.

[17] T. Shibata, M. Uenuma, T. Yamada, K. Yoshitsugu, M. Higashi, K. Nishimura, and Y. Uraoka, "Effects of carbon impurity in ALD-Al_2O_3 film on HAXPES spectrum and electrical properties of Al_2O_3/AlGaN/GaN MIS structure," *Jpn. J. Appl. Phys.*, vol. 61, no. 6, Jun. 2022, Art. no. 065502, doi: 10.35848/1347-4065/ac646d.

[18] R. Asahara, M. Nozaki, T. Yamada, J. Ito, S. Nakazawa, M. Ishida, T. Ueda, A. Yoshigoe, T. Hosoi, T. Shimura, and H. Watanabe, "Effect of nitrogen incorporation into Al-based gate insulators in AlON/AlGaN/GaN metal–oxide–semiconductor structures," *Appl. Phys. Exp.*, vol. 9, no. 10, Oct. 2016, Art. no. 101002, doi: 10.7567/apex.9.101002.

[19] H.-C. Wang, T.-E. Hsieh, Y.-C. Lin, Q. H. Luc, S.-C. Liu, C.-H. Wu, C. F. Dee, B. Y. Majlis, and E. Y. Chang, "AlGaN/GaN MIS-HEMTs with high quality ALD-Al_2O_3 gate dielectric using water and remote oxygen plasma as oxidants," *IEEE J. Electron Devices Soc.*, vol. 6, pp. 110–115, 2018, doi: 10.1109/JEDS.2017.2779172.

[20] M. Tajima, J. Kotani, and T. Hashizume, "Effects of surface oxidation of AlGaN on DC characteristics of AlGaN/GaN high-electron-mobility transistors," *Jpn. J. Appl. Phys.*, vol. 48, no. 2R, Feb. 2009, Art. no. 020203, doi: 10.1143/jjap.48.020203.

[21] S. Ozaki, T. Ohki, M. Kanamura, N. Okamoto, and T. Kikkawa, "Effect of atomic-layer-deposition method on threshold voltage shift in AlGaN/GaN metal–insulator–semiconductor high electron mobility transistors," *Jpn. J. Appl. Phys.*, vol. 52, no. 11S, Nov. 2013, Art. no. 11NG04, doi: 10.7567/jjap.52.11ng04.

[22] S. Huang, Q. Jiang, S. Yang, Z. Tang, and K. J. Chen, "Mechanism of PEALD-grown AlN passivation for AlGaN/GaN HEMTs: Compensation of interface traps by polarization charges," *IEEE Electron Device Lett.*, vol. 34, no. 2, pp. 193–195, Feb. 2013, doi: 10.1109/LED.2012.2229106.

[23] W.-C. Cheng, J. He, M. He, Z. Qiao, Y. Jiang, F. Du, X. Wang, H. Hong, Q. Wang, and H. Yu, "Low trap density of oxygen-rich HfO_2/GaN interface for GaN MIS-HEMT applications," *J. Vac. Sci. Technol. B, Microelectron.*, vol. 40, no. 2, Mar. 2022, doi: 10.1116/6.0001654.

[24] S. Yang, S. Liu, Y. Lu, C. Liu, and K. J. Chen, "AC-capacitance techniques for interface trap analysis in GaN-based buried-channel MIS-HEMTs," *IEEE Trans. Electron Devices*, vol. 62, no. 6, pp. 1870–1878, Jun. 2015, doi: 10.1109/TED.2015.2420690.

[25] S. Yang, Z. Tang, K.-Y. Wong, Y.-S. Lin, C. Liu, Y. Lu, S. Huang, and K. J. Chen, "High-quality interface in Al_2O_3/GaN/GaN/AlGaN/GaN MIS structures with in situ pre-gate plasma nitridation," *IEEE Electron Device Lett.*, vol. 34, no. 12, pp. 1497–1499, Dec. 2013, doi: 10.1109/LED.2013.2286090.

[26] X. Lu, K. Yu, H. Jiang, A. Zhang, and K. M. Lau, "Study of interface traps in AlGaN/GaN MISHEMTs using LPCVD SiN_x as gate dielectric," *IEEE Trans. Electron Devices*, vol. 64, no. 3, pp. 824–831, Mar. 2017, doi: 10.1109/TED.2017.2654358.

[27] H. Sun, M. Wang, R. Yin, J. Chen, S. Xue, J. Luo, Y. Hao, and D. Chen, "Investigation of the trap states and V_{TH} instability in LPCVD Si_3N_4/AlGaN/GaN MIS-HEMTs with an in-situ Si_3N_4 interfacial layer," *IEEE Trans. Electron Devices*, vol. 66, no. 8, pp. 3290–3295, Aug. 2019, doi: 10.1109/TED.2019.2919246.

[28] Q. Bao, S. Huang, X. Wang, K. Wei, Y. Zheng, Y. Li, C. Yang, H. Jiang, J. Li, A. Hu, X. Yang, B. Shen, X. Liu, and C. Zhao, "Effect of interface and bulk traps on the C–V characterization of a LPCVD-SiN_x/AlGaN/GaN metal–insulator–semiconductor structure," *Semicond. Sci. Technol.*, vol. 31, no. 6, Jun. 2016, Art. no. 065014, doi: 10.1088/0268-1242/31/6/065014.

[29] M. Choi, J. L. Lyons, A. Janotti, and C. G. Van de Walle, "Impact of carbon and nitrogen impurities in high-k dielectrics on metal-oxide-semiconductor devices," *Appl. Phys. Lett.*, vol. 102, no. 14, Apr. 2013, doi: 10.1063/1.4801497.

[30] Q. Zhou, L. Liu, A. Zhang, B. Chen, Y. Jin, Y. Shi, Z. Wang, W. Chen, and B. Zhang, "7.6 V threshold voltage high-performance normally-off Al_2O_3/GaN MOSFET achieved by interface charge engineering," *IEEE Electron Device Lett.*, vol. 37, no. 2, pp. 165–168, Feb. 2016, doi: 10.1109/LED.2015.2511026.

[31] T.-H. Hung, M. Esposto, and S. Rajan, "Interfacial charge effects on electron transport in III-nitride metal insulator semiconductor transistors," *Appl. Phys. Lett.*, vol. 99, no. 16, Oct. 2011, doi: 10.1063/1.3653805.

[32] Z. H. Liu, G. I. Ng, S. Arulkumaran, Y. K. T. Maung, K. L. Teo, S. C. Foo, and V. Sahmuganathan, "Improved two-dimensional electron gas transport characteristics in AlGaN/GaN metal–insulator–semiconductor high electron mobility transistor with atomic layer-deposited Al_2O_3 as gate insulator," *Appl. Phys. Lett.*, vol. 95, no. 22, Nov. 2009, doi: 10.1063/1.3268474.

[33] Y. Zhang, L. Xu, Y. Gu, H. Guo, H. Jiang, K. M. Lau, and X. Zou, "Dynamic characteristics of GaN MISHEMT with 5-nm in-situ SiN_x dielectric layer," *IEEE J. Electron Devices Soc.*, vol. 10, pp. 540–546, 2022, doi: 10.1109/JEDS.2022.3189819.

[34] J.-J. Zhu, X.-H. Ma, Y. Xie, B. Hou, W.-W. Chen, J.-C. Zhang, and Y. Hao, "Improved interface and transport properties of AlGaN/GaN MIS-HEMTs with PEALD-grown AlN gate dielectric," *IEEE Trans. Electron Devices*, vol. 62, no. 2, pp. 512–518, Feb. 2015, doi: 10.1109/TED.2014.2377781.

[35] M. Hua, Y. Lu, S. Liu, C. Liu, K. Fu, Y. Cai, B. Zhang, and K. J. Chen, "Compatibility of AlN/SiN_x passivation with LPCVD-SiN_x gate dielectric in GaN-based MIS-HEMT," *IEEE Electron Device Lett.*, vol. 37, no. 3, pp. 265–268, Mar. 2016, doi: 10.1109/LED.2016.2519680.

[36] Z. Tang, S. Huang, Q. Jiang, S. Liu, C. Liu, and K. J. Chen, "High-voltage (600-V) low-leakage low-current-collapse AlGaN/GaN HEMTs with AlN/SiN_x passivation," *IEEE Electron Device Lett.*, vol. 34, no. 3, pp. 366–368, Mar. 2013, doi: 10.1109/LED.2012.2236638.

[37] C. Deng, W.-C. Cheng, X. Chen, K. Wen, M. He, C. Tang, P. Wang, Q. Wang, and H. Yu, "Current collapse suppression in AlGaN/GaN HEMTs using dual-layer SiN_x stressor passivation," *Appl. Phys. Lett.*, vol. 122, no. 23, Jun. 2023, doi: 10.1063/5.0135074.

[38] K. Nishiguchi, S. Kaneki, S. Ozaki, and T. Hashizume, "Current linearity and operation stability in Al_2O_3-gate AlGaN/GaN MOS high electron mobility transistors," *Jpn. J. Appl. Phys.*, vol. 56, no. 10, Oct. 2017, Art. no. 101001, doi: 10.7567/jjap.56.101001.

[39] T. Kubo, M. Miyoshi, and T. Egawa, "Post-deposition annealing effects on the insulator/semiconductor interfaces of Al_2O_3/AlGaN/GaN structures on Si substrates," *Semicond. Sci. Technol.*, vol. 32, no. 6, Jun. 2017, Art. no. 065012, doi: 10.1088/1361-6641/aa6c09.

QIANG WANG received the M.S. degree from the North University of China, in 2021. He is currently pursuing the Ph.D. degree in electronic information with Fudan University. His current research interest includes optimizing the fabrication process for GaN devices.

MAOLIN PAN received the B.S. degree from Soochow University, in 2021. He is currently pursuing the Ph.D. degree in electronic information with Fudan University. His current research interest includes integration of GaN power devices.

PENGHAO ZHANG received the Ph.D. degree from Fudan University, in 2023. His current research interest includes etching process for GaN power devices.

LUYU WANG received the B.S. degree from Harbin Engineering University, in 2020. He is currently pursuing the Ph.D. degree in electronic information with Fudan University. His current research interest includes the fabrication of enhanced GaN power devices.

YANNAN YANG received the B.S. degree from Xi'an Jiaotong University, in 2020. She is currently pursuing the Ph.D. degree in microelectronics and solid state electronics with Fudan University. Her current research interest includes surface treatment of GaN power devices.

XINLING XIE received the B.S. degree from South China University, in 2021. She is currently pursuing the M.S. degree in microelectronics and solid state electronics with Fudan University.

HAI HUANG received the B.S. degree from the University of Electronic Science and Technology of China, in 2022. He is currently pursuing the M.S. degree in microelectronics and solid state electronics with Fudan University.

XIN HU received the B.S. degree from Wuhan University, in 2022. She is currently pursuing the M.S. degree in electronic information with Fudan University.

MIN XU received the Ph.D. degree in electrical engineering from Purdue University, in 2011. Currently, he is a Professor with the College of Microelectronics, Fudan University, Shanghai, China. His research interest includes the design of third-generation semiconductor power devices and their systems application.

• • •